Geodesic turnpikes for robot motion planning

Yann de Mont-Marin, Martial Hebert, Jean Ponce

Geodesic turnpikes for robot motion planning

Yann de Mont-Marin*†, Martial Hebert‡ and Jean Ponce†§
*Inria Paris, France
†Departement d'Informatique de l'ENS (CNRS, PSL Research University), France
‡Robotics Institute, School of Computer Science, Carnegie Mellon University, United States
§Courant Institue and Center for Data Science, New York University, United States
Corresponding mail: yann.de-mont-marin@inria.fr

***Abstract*—Endowing the configuration space of a robot with an appropriate metric structure and characterizing and computing the corresponding geodesics are central issues in motion planning. As recently observed in [1], the geodesics of $\mathrm{SE}(2)$ equipped with the so-called minimum swept-volume distance exhibit in practice a behavior akin to the *turnpike property* in optimal control, with transient phases separated by a longer steady state close to prototypical trajectories, the *turnpikes* [2]. This presentation gives a theoretical counterpoint to this empirical observation with a formal definition of geodesic turnpikes using vector fields on Finsler manifolds, a simple differential characterization of geodesics in the case where the manifold is a Lie group and the Finsler distance is left-invariant, and, in the case where the corresponding operator is also reversible, a conjecture characterizing the turnpikes by vector fields satisfying simple conditions in the corresponding Lie algebras. As a proof of concept, closed-form (resp. numerical) procedures for computing these vector fields according to this conjecture are given for $\mathrm{SE}(2)$ equipped with the left-invariant Riemannian (resp. minimum swept-volume) distance introduced in [3] (resp. [1]) for rectangular shapes. The solutions empirically match, in both cases, the observed turnpike behavior of the corresponding geodesics. In the minimum swept-volume distance case, using the turnpikes for initialization also yields an order-of-magnitude speedup in computing geodesics.**

I. Introduction

A. Context

The **configuration space** of a robot and the corresponding **forward kinematics** can be represented in many different ways, notably in terms of the associated **Lie group** and **Lie algebra** [4]. The choice of the **distance** function used to endow this space with a **metric structure** as well as the nature of the corresponding **geodesics** –that is, roughly speaking, the locally or globally shortest paths in that space– play a key role in planning the best possible motions in tasks such as grasping and manipulation or navigation in the presence of obstacles [5, 6, 7]. Conversely, this choice may be guided by various task heuristics, such as minimizing the chance of collision along a path [1, 8] or end-effector behavior [9].

Riemannian geometry and its **Finslerian generalization** provide a natural framework for constructing well-defined distances satisfying these heuristics and characterizing their geodesics. For example, Jaquier *et al.* [10, 11, 12] propose Riemannian geometry as a unifying framework for robot motion learning and control, Ratliff *et al.* [9, 13, 14] use Finsler geometry to model motion policies called "geometric fabrics". The calculation of geodesics is computationally challenging. Hence, simple metric structures, for which closed forms are available, are employed today, although they offer limited possibilities for integrating heuristics. To use distances that integrate heuristics, we need to leverage properties that accelerate the computation of geodesics.

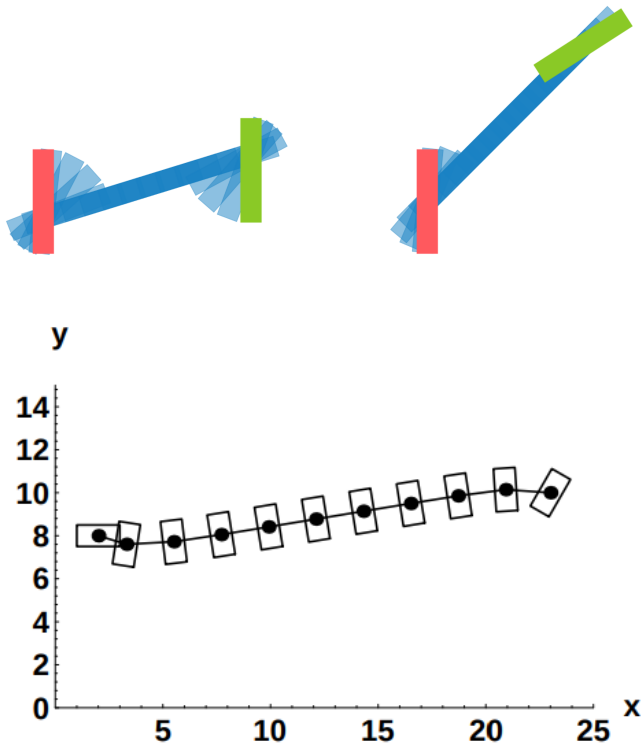

Fig. 1. Geodesics on $\mathrm{SE}(2)$ for a rotating and translating rectangle under **(top)** the minimum swept-volume distance proposed in [1] and **(bottom)** [3, Fig. 3(c)] a left-invariant Riemannian distance proposed in [3]. Reprinted with permission from [1, 3]. Copyright © 1998, 2023, IEEE. In both cases, the behavior of geodesics hints at a turnpike phenomenon.

Figure 1 shows the geodesics joining two configurations of a rectangle rotating and translating in the plane associated with two distances over $\mathrm{SE}(2)$, the Finslerian minimum swept-volume distance proposed in de Mont-Marin *et al.* [1] (Fig. 1(top)), and, a Riemannian distance introduced in Žefran *et al.* [3] (Fig. 1(bottom)). In both cases, the motion along the trajectory is (essentially), except near its endpoints, a pure translation parallel to the long side of the rectangle in the Finslerian case and parallel to the short side in the

Riemannian one. This behavior, where geodesics appear to stay close to simpler prototypical trajectories, except for short transient phases, is reminiscent of the **turnpike phenomenon** in optimal control [2, 15, 16]. Indeed, it can be shown that, for certain optimal control problems with a sufficiently large time horizon, any optimal trajectory remains, for most of the time, close to a **turnpike**, that is, the optimal solution of an associated stationary optimal control problem [2, 16]. In this setting, any optimal trajectory can be decomposed into three segments: it first converges exponentially fast from its start point to the turnpike, then spends most of its time there, and finally converges exponentially fast to its endpoint. Trélat and Zuazua demonstrate in [2, 17] that turnpikes can be used to initialize optimal control problems and significantly accelerate their computation.

To the best of our knowledge, the apparent turnpike behavior in Fig. 1 has not been formalized for Riemannian and Finslerian distance in the literature. Nor has it been exploited in the efficient computation of geodesics. We introduce in this paper a framework for **geodesic turnpikes**. It involves identifying a vector field, called the geodesic turnpike, and showing that geodesic velocities are close to that field for most of the geodesic length.

In section II, we clarify the mathematical background of distance, metric structure, geodesics, and Finsler geometry, and in section III, following a similar construction done in [16] for the optimal control setting, we introduce the framework for *geodesic turnpike* of a Finsler distance. Subsequently, in Proposition 6, we propose a new Lie algebra formulation of the geodesic equation for left-invariant Finsler distances on Lie groups, and we leverage this formulation with classical tools from dynamical systems [18] to propose a conjecture on the conditions for a left-invariant vector field to be a geodesic turnpike for a left-invariant Finslerian distance. In section IV-B, we give a proof of concept of the conjecture usage to find the vector fields for the examples illustrated in Fig. 1: analytically for the Riemannian distance on $\mathrm{SE}(2)$ proposed in [3] (Fig. 1(bottom)) and numerically for the minimum swept-volume distance proposed in [1] (Fig. 1(top)). In both cases, the vector fields match the turnpike behavior observed. For the minimum swept-volume distance, we use the vector fields to initialize a geodesic solver and observe an order of magnitude speed-up.

Our main contributions are:

1) A formal definition of geodesics turnpikes on Finsler manifolds.
2) A geodesic equation for left-invariant Finsler distances on Lie groups.
3) A conjecture for a sufficient condition for a left-invariant vector field to be a geodesic turnpike for a left-invariant Finsler distance.
4) A proof of concept of geodesic computation acceleration using geodesic turnpikes for initialization.

B. Related work

Metric structures on configuration space. Many non-canonical metric structures on the configuration space have been extensively explored. For instance, in [19], Zhang *et al.* study the maximum vertex distance, previously proposed by Lavalle [6]. In [1], the authors construct the minimum swept-volume distance that reduces collision probabilities along geodesics. An advantage of the latter is its compatibility with the Finslerian formalism, which allows it to benefit from the treatment proposed in this paper.

Žefran *et al.* provide in [20, 3] a comprehensive examination of Riemannian geometries on the configuration space of a solid, establishing properties necessary for a geometric structure to adhere to fundamental principles of mechanics. However, their study is confined to the case of a configuration space isomorphic to $\mathrm{SE}(3)$ and lacks insights for practical implementations.

Turnpikes. Turnpike properties have a long-standing history in finite-dimensional optimal control problems within econometrics [15]. Trélat and Zuazua conducted in-depth investigations, introducing exponential turnpikes that provide a strong bound on the proximity between a trajectory and its turnpike [2]. Sakamoto and Zuazua [16] reformulated essential turnpike properties in optimal control using geometric and dynamical system tools, significantly influencing our current work. Faulwasser *et al.* introduced the concept of a velocity turnpike in [21], where the turnpike is characterized not as a position but by the steadiness of the velocity. However, this notion needs to be revised for characterizing a turnpike behavior for geodesics, given the inherent invariance in the problem as discussed in section II. Turnpikes in robotics are closely related to the trim primitives studied in [22].

II. Geometry background

A. Metric spaces

Consider some metric space (X,d) defined by a set X and a distance function $d : X^2 \to \mathbb{R}^+$. Let $I = [a,b]$ denote some interval of the real line and, given some positive integer N, let $\sigma_N(I)$ denote the set of all sequences $t = \{t_0, t_1, \ldots, t_N\}$ of size $N+1$ such that $a = t_0 < t_1 < \ldots < t_N = b$. Given a continuous parametric curve $\gamma : I \to X$, we define its *length* $L(\gamma)$ as

$$L(\gamma) = \sup_{N \in \mathbb{N}^*, t \in \sigma_n(I)} \sum_{i=0}^{N-1} d(\gamma(t_{i+1}), \gamma(t_i)). \tag{1}$$

We say that γ is a rectifiable parametric curve when $L(\gamma)$ is finite.

Given a parametric curve $\gamma : I \to X$ and some interval J, a continuous and monotone map $\phi : I \to J$, $\gamma \circ \phi$ is called a *reparameterization* of γ. The image of a parametric curve, $\gamma(I) \subset X$, is invariant to parameterization: $\gamma(I) = \gamma \circ \phi(J)$, and the length of a curve $L(\gamma)$ is also invariant to parameterization: $L(\gamma) = L(\gamma \circ \phi)$. The set of all reparameterizations of a parametric curve forms an equivalence class, the *geometric curve*, with a well-defined length. We say that a parametric curve *represents* the corresponding geometric curve. From

now on, we assume that all parametric curves of interest are defined over $I = [0,1]$, thanks to the length invariance to reparameterization.

We say that a rectifiable parametric curve γ represents a *geodesic* when for any $t < t'$ in I we have

$$L(\gamma|_{[t,t']}) = d(\gamma(t), \gamma(t')). \tag{2}$$

A *geodesic* is a geometric curve for which length and distance coincide on every curve segment. A parametric curve γ represents a *local geodesic* if, for any t in I there exists some $\varepsilon > 0$ such that $\gamma|_{[t-\varepsilon,t+\varepsilon]}$ represents a geodesic. Every geodesic is a local geodesic. For a geodesic (resp. local geodesic), there exists a unique parametric curve $\gamma : [0,1] \to X$ representing the geodesic (resp. local geodesic) with *constant velocity*, i.e., for every t in $[0,1]$ we have

$$L(\gamma|_{[0,t]}) = t d(\gamma(0), \gamma(1)), \tag{3}$$

which provides a canonical representative of the geodesic.

We say that (X,d) is a geodesic space if, for any pair of points x, y, a geodesic joining those points exists. Let $C^0(x,y)$ denote the set of all continuous parametric curves joining x and y; the so-called Hopf-Rinow theorem gives the conditions on the existence of geodesic spaces.

Theorem 1 (Hopf-Rinow theorem)**.** *Let (X,d) denote a complete and locally compact metric space such that for any pair of points x, y, there exists a rectifiable curve joining those points. The inner distance, denoted by d_i, is defined as*

$$d_i(x,y) = \inf_{\gamma \in C^0(x,y)} L(\gamma), \tag{4}$$

is well defined and (X,d_i) is a geodesic space. The lengths defined by d and d_i are equal.

The inner-distance construction (4) shows how to construct a geodesic space from a metric space. It is, for example, the construction of the minimum swept-volume distance presented in [1]. We assume from now on that (X,d) is a geodesic space with $d_i = d$ as configuration space distances in robotics usually satisfy the hypothesis of Theorem 1.

If in addition X is a C^∞ manifold and d is C^∞, we define the Finsler operator F by, for any x in X and v in T_xX the tangent space to X in x:

$$F(x,v) = \lim_{\varepsilon \to 0^+} \frac{1}{\varepsilon} d(\gamma(0), \gamma(\varepsilon)) = \lim_{\varepsilon \to 0^+} \frac{1}{\varepsilon} L\left(\gamma|_{[0,\varepsilon]}\right), \tag{5}$$

with any C^∞ parametric curve $\gamma : [0,1] \to X$ such that $\gamma(0) = x$ and $\dot{\gamma}(0) = v$. The construction is independent of the choice of γ, and we say that (X,F) is a Finsler manifold. We refer the reader to Bucataru [23] for an extended introduction to Finsler geometry. In particular, F is C^∞ and for any x in X, the map $v \in T_xX \to F(x,v)$ is a norm on T_xX. We assume from now on that all parametric curves of interest are C^∞.

B. Finsler geodesics

Let us assume from now on that (X,F) is a C^∞ Finsler manifold of dimension n with the associated distance d. As shown in [23] for example, the length of a parametric curve γ defined on $[0,1]$ with endpoints, $x_0 = \gamma(0)$ and $x_1 = \gamma(1)$ verifies

$$L(\gamma) = \int_0^1 F(\gamma(t), \dot{\gamma}(t)) dt. \tag{6}$$

Property 2 ([23])**.** *The global (resp. local) minimizers of L among all parametric curves joining x_0 to x_1 represent geodesics (resp. local geodesics) joining these two points.*

It is also convenient to define the *energy* function associated with the parametric curve γ as

$$E(\gamma) = \frac{1}{2} \int_0^1 F^2(\gamma(t), \dot{\gamma}(t)) dt. \tag{7}$$

Property 3 ([23])**.** *The global (resp. local) minimizers of E among all parametric curves joining x_0 to x_1 represent the local geodesics (resp. geodesics) between these two points with* constant velocity*. A geodesic joining x_0 to x_1 has one and only one representative that is also a minimizer of E. The minimizers of E are canonical representatives for the geodesics joining x_0 to x_1. A minimizer of E is also a minimizer of L, and the converse is true if and only if the parametric curve has constant velocity.*

A minimizer γ^* of E joining x_0 to x_1 is also a minimizer of L and has constant velocity. Thus, there exists C such that $F(\gamma^*(t), \dot{\gamma}^*(t)) = C$ for any t in $[0,1]$. Substituting C in both (6) and (7) yields

$$2E(\gamma^*) = L(\gamma^*)^2 = d(x_0,x_1)^2. \tag{8}$$

In addition, with the re parametrization $\phi : [0, d(x_0,x_1)] \to [0,1]$ such that $\phi(t) = \frac{t}{d(x_0,x_1)}$, we denote by $\gamma^\dagger = \gamma^* \circ \phi$, defined on $[0, d(x_0,x_1)]$, the unique curvilinear parametric curve representing the geodesic. For all t in $[0, d(x_0,x_1)]$ we have

$$F\left(\gamma^\dagger(t), \dot{\gamma}^\dagger(t)\right) = 1. \tag{9}$$

In the rest of the paper, γ^* is always defined on $[0,1]$ and is a minimizer of the energy E, and $\gamma^\dagger$ is always a curvilinear parametrization of γ^*.

Using the minimizers of E provides a unique representation of the geodesics. Perhaps more importantly, E can be used to characterize the geodesics by a differential equation. For this purpose, we introduce the fundamental bilinear form associated with the Finsler operator F. For any (x,v) in TX we define the bilinear form $g(x,v)$ on T_xX by, for any a and b in T_xX:

$$g(x,v)(a,b) = \frac{1}{2} \frac{\partial^2}{\partial s \partial t} F^2(x, v + sa + tb) \bigg|_{s=0,t=0}. \tag{10}$$

Using the Euler-Lagrange equation from the calculus of variation, we obtain a new characterization of the geodesics.

Property 4 (Geodesic equation [23])**.** *The differential equation is written in local coordinates using Einsteinian notation for l in $1..n$ as*

$$g_{il}\ddot{\gamma}^i + \frac{1}{2}\left(\frac{\partial g_{lj}}{\partial x^k} + \frac{\partial g_{lk}}{\partial x^j} - \frac{\partial g_{jk}}{\partial x^l}\right)\dot{\gamma}^j\dot{\gamma}^k = 0, \qquad (11)$$

where the dependency in γ and $\dot{\gamma}$ of g is left implicit for conciseness.

A necessary and sufficient condition for a C^∞ parametric curve γ to have constant velocity and represent a local geodesic is to be a solution of the geodesic equation.

A minimizer of E $\gamma^* : [0,1] \to X$ joining x_0 to x_1 and its curvilinear parameterization $\gamma^\dagger : [0, d(x_0,x_1)] \to X$ represent the same geodesic and have constant velocity, hence are solutions of the geodesic equation.

The bilinear form g is a cornerstone in the study of local geodesics and enjoys several properties inherited from the homogeneity of F. In particular, for (x,v) in TX, we have:

- $F^2(x,v) = g(x,v)(v,v)$.
- For any $\lambda > 0$, $g(x,\lambda v) = g(x,v)$.
- For any w in T_xX, $\frac{1}{2}\frac{\partial}{\partial s}F^2(x,v+sw)\Big|_{s=0} = g(x,v)(v,w)$.

Part of these results are given in [23], however for completeness of the paper, proofs of the results crucial for Proposition 6 of the next section are presented in Appendix A.

III. Lie groups and geodesic turnpikes

A. Motivation for robotic applications

In robotics, the configuration space is often a Lie Group. For example, for a free-flying robot, the configuration space is $X = \mathrm{SE}(3)$ the group of rigid placements, and for a serial manipulator arm with six joints, it is $X = \mathrm{SO}(2)^6$. Those spaces are always equipped with a smooth Finsler operator. For example, $\mathrm{SE}(3)$ is generally equipped with the left-invariant canonical Riemannian distance [24] for which the geodesics have a closed form. For more complex distances, such as the minimum swept-volume distance in [1], the geodesics are not available in closed form and must be computed efficiently. We need to solve the problem

$$\min_{\gamma \in \mathcal{C}^\infty([0,1],X)} \frac{1}{2}\int_0^1 F^2(\gamma(t),\dot{\gamma}(t))dt, \qquad (12)$$
$$\text{s.t.} \quad \gamma(0) = x_0 \quad \text{and} \quad \gamma(1) = x_1,$$

for any x_0 and x_1 in X.

On the one hand, one can solve a discretized version of (12) using off-the-shelf minimization software such as [25, 26]. On the other hand, one can solve (12) using a bounded value ODE solver, such as [27] with the induced geodesic equation (11) and boundary conditions $\gamma(0) = x_0$ and $\gamma(1) = x_1$. In both cases, however, the initialization has a crucial impact on the performance of the algorithms because the underlying numerical minimization problems are not necessarily convex.

The geodesics of [1, 3], illustrated in Fig. 1, suggest a turnpike behavior. To the best of our knowledge, this behavior has not been formalized nor used to improve the computation of solutions of (12). We propose formalizing this behavior in terms of *geodesic turnpike* using vector fields. We can initialize geodesic solvers efficiently using these vector fields as presented in section IV-B.

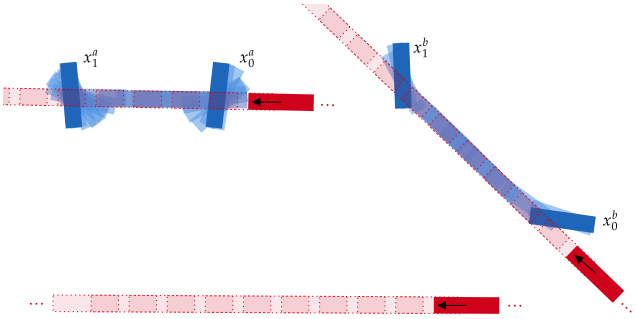

Fig. 2. Illustration of geodesic turnpikes. In blue, we plot two Finslerian geodesics of the minimum swept-volume distance [1], joining x_0^a with x_1^a and x_0^b with x_1^b. In red, we plot three integral curves of V, the vector field of instantaneous translations on the small side illustrated by the black arrow. We observe that for each geodesic, there exists an integral curve of V that approximates the geodesic well except at its start and end points.

B. Geodesic turnpike definition

Let (X,F) denote a Finsler manifold, and d denote the associated distance. Let V denote a smooth vector field on X. Qualitatively, V is a geodesic turnpike for F on X if every curvilinear parametrization $\gamma^\dagger$ of a geodesic has its derivative $\dot{\gamma}^\dagger$ *"close"* to V. Figure 2 illustrates the idea, with $X = \mathrm{SE}(2)$, F the operator for the minimum swept-volume distance [1] and V the vector field of instantaneous translation on the small side, illustrated with a black arrow. We observe that for each geodesic, there exists an integral curve of V that approximates the geodesic well except near its start and end points.

To formalize the notion of *"close"*, we propose a definition of *exponential geodesic turnpike* inspired by exponential turnpikes in the context of optimal control [2].

Definition 1 (Exponential geodesic turnpike)**.** *We say that a smooth vector field V is an exponential geodesic turnpike for F on X if there exist constants $K > 0$ and $\sigma > 0$ such that for any x_0, x_1 in X and any curvilinear parametrization $\gamma^\dagger : [0, d(x_0,x_1)] \to X$ of a geodesic joining x_0 and x_1 we have for all t in $[0, d(x_0,x_1)]$:*

$$F\left(\gamma^\dagger(t), \dot{\gamma}^\dagger(t) - V_{\gamma^\dagger(t)}\right) \leq K\left(e^{-\sigma t} + e^{-\sigma(d(x_0,x_1)-t)}\right). \qquad (13)$$

The left-hand side of Eq. (13) is the distance between $\dot{\gamma}^\dagger(t)$ and $V_{\gamma^\dagger(t)}$ because the mapping $v \mapsto F(x,v)$ is a norm on T_xX. The right-hand side of Eq. (13) is an exponential upper bound. The bound is loose for t near 0 due to the first term of the right-hand side and for t near $d(x_0,x_1)$ due to the second term of the right-hand side. The bound tightens exponentially when t is far from the boundaries of $[0, d(x_0,x_1)]$. Figure 3 illustrates this behavior for a minimum swept-volume distance geodesic [1]. In the proposed formalism, the turnpike is a vector field, and the bound is in the space of velocities. In this sense, it resembles the velocity turnpikes [21]. In addition, the bound on the velocity $\dot{\gamma}^\dagger$ induces a bound on $\gamma^\dagger(t)$ by integration.

The bound on $\gamma^\dagger(t)$ is not explored in the present framework and is left for future work.

It is important to note that K and σ do not depend on x_1 and x_2, and thus the upper bound in Definition 1 do not depend on x_1 and x_2, but only on the distance $d(x_0,x_1)$ between those points. It implies that with a given precision, the length of the geodesic segment for which the velocity bound (13) is looser than ε does not depend on the total geodesic length.

Proposition 5. *For any $\varepsilon > 0$, there exists $\tau > 0$ such that for any curvilinear parametric curve $\gamma^\dagger$ representing a geodesic, if I_ε denote the interval of t such that $F\left(\gamma^\dagger(t), \dot\gamma^\dagger(t) - V_{\gamma^\dagger(t)}\right) \geq \varepsilon$ we have*

$$L\left(\gamma^\dagger|_{I_\varepsilon}\right) \leq \tau. \tag{14}$$

The proof is given in Appendix B and Fig. 4 illustrates this proposition. Proposition 5 ensures that an integral curve of V near x_0 and x_1 is a good approximation of L. Moreover, the larger L is, the better the approximation is since $\tau/L \to 0$ as $L \to \infty$. In the example illustrated in Fig. 1, even configurations that appear "close" in the workspace have a "large" geodesic length from the point of view of the turnpike property.

C. Left-invariant Finsler operators on Lie groups

We now study the case of invariant reversible Finsler distance on Lie groups to identify sufficient conditions for the geodesic turnpike property. From now on, X is a Lie group.

Given some h in X, we denote by $\tilde L_h$ the left tangent action (see the book of Chirikjian [28] for further details on Lie groups). For any x in X, $\tilde L_h$ is a linear map between the tangent space T_xX onto, the tangent space $T_{h\circ x}X$. We say that F is left-invariant on X, if for every (x,v) in TX and h in X,

$$F(x,v) = F(h\circ x, \tilde L_h v), \tag{15}$$

i.e., the Finsler operator does not change when we compose x on the left with a group element h, and we compose v with the associated tangent map. In particular, with $h = x^{-1}$, we have $F(x,v) = F(e, \tilde L_{x^{-1}} v)$ where e denote the identity element of X. Let $C(u) = \frac{1}{2}F^2(e,u)$ denote the cost function used in (12) restricted on the Lie algebra $\mathfrak{X}$ and let $u : [0,1] \to \mathfrak{X}$ such that $\dot\gamma(t) = \tilde L_{\gamma(t)} u(t)$, then (12) is equivalent to

$$\min_{\gamma \in \mathcal{C}^\infty([0,1],X), u \in \mathcal{C}^\infty([0,1],\mathfrak{X})} \int_0^1 C(u(t))dt, \tag{16}$$

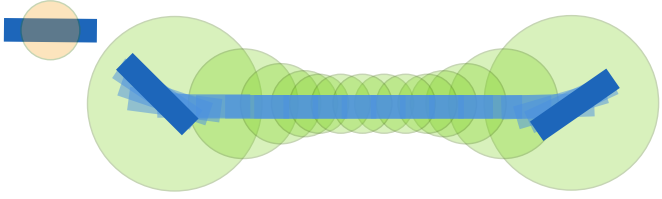

Fig. 3. Illustration of an exponential geodesic turnpike bound for a geodesic of the minimum swept-volume distance [1]. For visualization purposes, we attach a disc in orange to the rectangle in blue. The exponential bound in Definition 1 induces a maximum displacement of the orange disc along the geodesic. The union of the resulting varying radius discs in green is an upper bound of the workspace region guaranteed by the exponential bound for the attached disc.

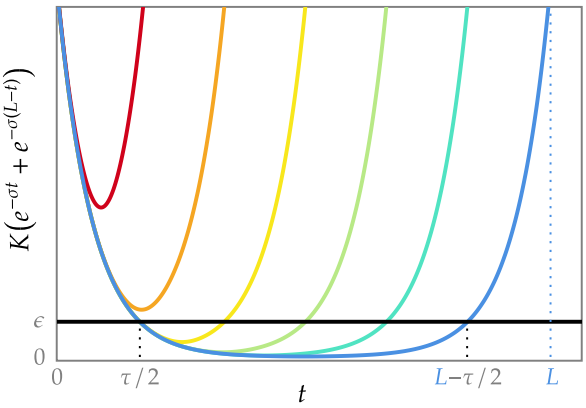

Fig. 4. To illustrate Proposition 5, we plot the exponential bound (13) as a function of the curvilinear abscissa t of geodesics of various lengths. Even for longer geodesics, the bound is upper-bounded by ε whenever $\tau/2 < t < L - \tau/2$. The first two curves (red and orange) correspond to geodesics with lengths lower than τ.

$$\begin{aligned} \text{s.t} \quad & \forall t \in [0,1], \quad \dot\gamma(t) = \tilde L_{\gamma(t)} u(t), \\ & \gamma(0) = x_0, \\ & \gamma(1) = x_1. \end{aligned}$$

We now use the calculus of variations to obtain a more tractable geodesic equation associated with (16)

Proposition 6. *If F is a left-invariant Finsler distance on the Lie group X, then the geodesic equation associated to* (16) *can be written in some basis of $\mathfrak{X}$:*

$$\begin{aligned} \dot\gamma(t) &= \tilde L_{\gamma(t)} u(t), \\ \dot u(t) &= G_{u(t)}^{-1} \operatorname{ad}_{u(t)}^\top G_{u(t)} u(t), \end{aligned} \tag{17}$$

where G_u denote the matrix representation of $g(e,u)$ in the chosen basis and ad_u denote the matrix representation of the adjoint operator of u on $\mathfrak{X}$ in the chosen basis. The solutions represent local geodesics and do not depend on the basis choice.

The proof can be found in Appendix C. In the Riemannian case, G_u is independent of u, and we recover the so-called Euler-Arnol'd equation [29]. We feel that Proposition 6 should be textbook material since it resembles classical results such as [30, 31] but, to the best of our knowledge, this geodesic equation for invariant Finsler distances has not been written in this form yet.

D. Geodesic turnpikes for left-invariant Finsler distances

Let us now study the dynamics given by the geodesic equation (17) of the left-invariant Finsler operator F on X. The objective is to construct a vector field V that is an exponential geodesic turnpike for F on X as defined in Definition 1. Any curvilinear parametrization $\gamma^\dagger$ defined on $[0,L]$ and representing a geodesic is a solution of the geodesic equation (17). In other words, $u(t) = \tilde L^{-1}_{\gamma^\dagger(t)} \dot\gamma^\dagger(t)$ is a solution of the dynamics $\dot u = D(u)$ where D denote the dynamics function

on the lie algebra $\mathfrak{X}$: $D(u) = G_u^{-1} \operatorname{ad}_u^\top G_u u$. The solutions of the geodesic equation have constant velocity and $\gamma^\dagger(t)$ is a curvilinear parametrization, so we have for any t in $[0,L]$, $F(e,u(t)) = F(\gamma^\dagger(t), \dot\gamma^\dagger(t)) = 1$. Thus, the dynamical system $\dot u = D(u)$ is well defined on $S_F(1)$ the set of all u in $\mathfrak{X}$ defined by $F(e,u) = 1$. We study the dynamics associated with D on $S_F(1)$.

The lie algebra elements $\bar u$ in $S_F(1)$ verifying $D(\bar u) = 0$ are the *equilibrium points* of the dynamics on $S_F(1)$. Equivalently $\bar u$ satisfies

$$\operatorname{ad}_{\bar u}^\top G_{\bar u} \bar u = 0, \quad \bar u^\top G_{\bar u} \bar u = 1, \tag{18}$$

as detailed in Appendix D. The matrix $\operatorname{ad}_u^\top$ is a linear endomorphism of $\mathfrak{X}$ and the mapping $u \mapsto \operatorname{ad}_u^\top$ is linear in u. We denote by P_u the unique matrix defined by

$$\forall v \in \mathfrak{X}, \quad \mathrm{P}_u v = \operatorname{ad}_v^\top u. \tag{19}$$

We prove in Appendix D that the Jacobian J of the dynamics D taken in an equilibrium point $\bar u$ is

$$J_{\bar u} = G_{\bar u}^{-1} (\operatorname{ad}_{\bar u}^\top G_{\bar u} + \mathrm{P}_{G_{\bar u} \bar u}). \tag{20}$$

The dynamics around the equilibrium point are given by the spectrum of $J_{\bar u}$ (see [18]). As we study the dynamics on $S_F(1)$, we restrict the Jacobian to the tangent space $A = T_{\bar u} S_F(1)$ and we prove in Appendix D that A is exactly the vector space of elements v in $\mathfrak{X}$ such that $v^\top G_{\bar u} \bar u = 0$.

Definition 2 (Saddle point on the unit sphere)**.** *An equilibrium point $\bar u$ of our dynamics D on $S_F(1)$ is called a saddle point if the eigenvalues of the endomorphism $J_{\bar u}|_A$ have non-null real parts and at least one eigenvalue has a positive real part, and one eigenvalue has a negative real part.*

The theory of dynamical systems [18] gives a general characterization of saddle points. Sakamoto *et al.* [16] sums up many of those results, with particular attention to the existence of exponential bounds for a dynamical system around saddle points. In our settings, we say that a sub-manifold M of $S_F(1)$ is an invariant sub-manifold if any solution of the dynamics $\dot u = D(u)$ with $u(0)$ in M, remains in M for all time t. Let $\bar u$ denote a saddle point on the unit sphere and m denote the dimension of $S_F(1)$. The theory of dynamical systems [18] states that there exists an invariant sub-manifold U of $S_F(1)$ of dimension k tangent to the eigenvectors of $J_{\bar u}|_A$ associated with negative eigenvalues called the *unstable manifold* and an invariant sub-manifold S of $S_F(1)$ of dimension $m-k$ tangent to the eigenvectors of $J_{\bar u}|_A$ associated with positive eigenvalues called the *stable manifold*. Sakamoto *et al.* prove the following theorem

Theorem 7 (Theorem 3 in [16])**.** *For any u_0 in S, any u_1 in U, any $(m-k)$-dimensional disc $\overline{D}$ transversal to S at u_0, and any k-dimensional disc $\overline{E}$ transversal to U at u_1, there exist constants $T_0 > 0$, $K > 0$ and $\sigma > 0$ such that for every $T > T_0$, there exists a $\rho > 0$, v_0 in $B(u_0,\rho) \cap \overline{D}$ and v_1 in $B(u_1,\rho) \cap \overline{E}$ such that there exists a solution u^* of the dynamics D such that $u^*(0) = v_0$ and $u^*(T) = v_1$ and for any t in $[0,T]$:*

$$\|u^*(t) - \bar u\| \leq K \left(e^{-\sigma t} + e^{-\sigma(T-t)} \right), \tag{21}$$

with $u \to ||u||$ a Euclidean norm on $\mathfrak{X}$. Moreover, $\rho \to 0$ when $T \to \infty$.

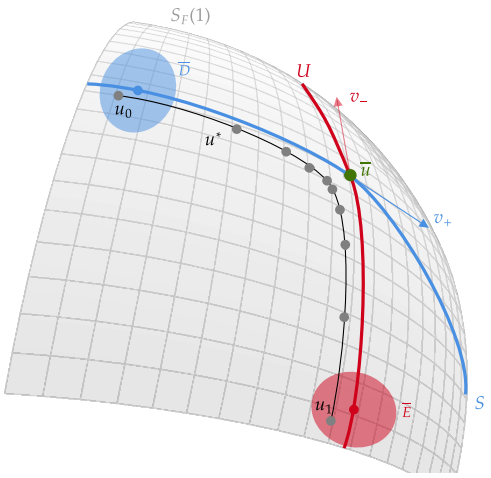

Fig. 5. Illustration of Theorem 7. We plot a portion of the surface $S_F(1)$ around a saddle point $\bar u$ of the Lie algebra dynamics $\dot u = D(u)$. We show an eigenvector v_+ associated with a positive eigenvalue tangent to the stable manifold S and, in red, an eigenvector v_- associated with a negative eigenvalue tangent to the unstable manifold U. We plot the transversal discs $\overline{D}$ and $\overline{E}$ near the stable and unstable manifolds. A solution u^* of the dynamics with $u^*(0) = u_0$ in $\overline{D}$ and $u^*(T) = u_1$ in $\overline{E}$ is illustrated in black and verify conditions of Theorem 7. The distance $\|u^*(t) - \bar u\|$ is exponentially bounded, as in (21). We illustrate with dots $u^*(t_i)$ for $i = 0..9$ where the sequence $t_i = iT/9$ form a regular partition of $[0,T]$. The distribution of the samples $u^*(t_i)$ illustrates the behavior induced by the exponential bound: u^* goes quickly toward the saddle point, slows down near it, and finishes fast toward the endpoint u_1.

This theorem is illustrated by Fig. 5. We now suppose that the set of all possible initial (resp. final) conditions on u_0 (resp. u_1) induced by the geodesic problem (16) satisfies the hypothesis of Theorem 7. In that case, constants $K > 0$ and $\sigma > 0$ guarantee an exponential bound on $\|u^*(t) - \bar u\|$. We have yet to prove that these assumptions are always satisfied in the case of a geodesic problem, and we leave this proof for future work. Nonetheless, we propose the following conjecture,

Conjecture 1. *Let F denote a left-invariant reversible Finsler operator on the Lie group X. Let $\bar u$ in $\mathfrak{X}$ verifying*

$$\operatorname{ad}_{\bar u}^\top G_{\bar u} \bar u = 0, \quad \bar u^\top G_{\bar u} \bar u = 1, \tag{18}$$

Let A denote the vector space of elements v in $\mathfrak{X}$ defined by $v^T G_{\bar u} \bar u = 0$ and $J_{\bar u}$ denote the matrix

$$J_{\bar u} = G_{\bar u}^{-1} (\operatorname{ad}_{\bar u}^\top G_{\bar u} + \mathrm{P}_{G_{\bar u} \bar u}). \tag{20}$$

If every eigenvalue of the endomorphism $J_{\bar u}|_A$ has a nonzero real part with at least one positive and one negative eigenvalue, then the left-invariant vector field $V_x = \tilde L_x \bar u$ is an exponential geodesic turnpike for the Finsler distance associated with F on X.

Indeed, if $\bar u$ is a saddle point as defined in Definition 2, and the assumptions regarding the validity of Theorem 7 discussed earlier are satisfied, then for any curvilinear parametrization

$\gamma^\dagger$ of a geodesic connecting x_0 and x_1, Theorem 7 with $T = d(x_0,x_1)$ implies that for all t in $[0,d(x_0,x_1)]$

$$\left\| \tilde{L}^{-1}_{\gamma^\dagger(t)} \dot{\gamma}^\dagger(t) - \bar{u} \right\| \leq K \left(e^{-\sigma t} + e^{-\sigma(d(x_0,x_1)-t)} \right). \tag{22}$$

The mapping $u \mapsto F(e,u)$ is a norm on $\mathfrak{X}$, and all norms are equivalent on a finite-dimensional vector space, so there exists $K' > 0$ such that for all u in $\mathfrak{X}$, we have $F(e,u) \leq K'\|u\|$. Using the left-invariance of F (15) with $h = \gamma^\dagger(t)$, we obtain

$$F\left(\gamma^\dagger(t), \dot{\gamma}^\dagger(t) - \tilde{L}_{\gamma^\dagger(t)} \bar{u} \right) \leq KK' \left(e^{-\sigma t} + e^{-\sigma(d(x_0,x_1)-t)} \right),$$

and the vector field $V_x = \tilde{L}_x \bar{u}$ is an exponential geodesic turnpike for F on X.

The following section presents a proof of concept of Conjecture 1 usage to analyze the examples given in Fig. 1.

IV. Exploration of conjecture 1 with examples

A. Geodesic turnpikes for a simple Riemannian distance

We study the existence of a geodesic turnpike for a simple left-invariant Riemannian metric structure on $\mathrm{SE}(2)$. We use an example proposed by Žefran in [3] as illustrated in Fig. 1(bottom). The detailed derivations are given in Appendix E.

Let $X = \mathrm{SE}(2)$ be the group of rigid transformation of $\mathbb{R}^2$, and $\mathfrak{X} = \mathfrak{se}(2)$ the Lie algebra of instantaneous motions. We denote by v_x, v_y and ω the three coordinates of an element u in the canonical basis of $\mathfrak{se}(2)$. With a slight abuse of notations, we write $u = [v_x, v_y, \omega]$. The left-invariant Riemannian operator used by Žefran to generate the geodesic in Fig. 1(bottom) is $F(e,u) = \sqrt{u^\top G u}$ with

$$G = \begin{bmatrix} \alpha & 0 & 0 \\ 0 & 1 & 0 \\ 0 & 0 & 1 \end{bmatrix}, \tag{23}$$

where $\alpha > 1$.

The matrices representation of ad_u and $\mathrm{P_u}$ in the canonical basis of $\mathfrak{se}(2)$ are

$$\mathrm{ad}_u = \begin{bmatrix} 0 & -\omega & v_y \\ \omega & 0 & -v_x \\ 0 & 0 & 0 \end{bmatrix} \quad \text{and} \quad \mathrm{P}_u = \begin{bmatrix} 0 & 0 & v_y \\ 0 & 0 & -v_x \\ -v_y & v_x & 0 \end{bmatrix}. \tag{24}$$

Let us recall that for a Riemannian distance $G_u = G$, so

$$\mathrm{ad}_u^\top G_u u = \begin{bmatrix} v_y \omega \\ -\alpha v_x \omega \\ (\alpha-1) v_x v_y \end{bmatrix}. \tag{25}$$

An equilibrium point $\bar{u}$ satisfies $\mathrm{ad}_u^\top G_u u$. Since $\alpha - 1 \neq 0$, (25) implies that at least two components of $\bar{u}$ must be zero. Using the fact that an equilibrium point also satisfies $\bar{u}^\top G_{\bar{u}} \bar{u} = 1$ we obtain exactly six equilibrium points on $S_F(1)$

$$\begin{aligned} &\bar{u}_1 = \alpha^{-1/2} e_1, \quad &&\bar{u}_2 = e_2, \quad &&\bar{u}_3 = e_3, \\ &\bar{u}_4 = -\alpha^{-1/2} e_1, \quad &&\bar{u}_5 = -e_2, \quad &&\bar{u}_6 = -e_3, \end{aligned} \tag{26}$$

where (e_1, e_2, e_3) is the canonical basis of $\mathfrak{se}(2)$.

We now calculate the Jacobian for these six equilibrium points to find the saddle points. Substituting (23) and (24) in the expression of J_u, (20), we obtain

$$J_u = \begin{bmatrix} 0 & \omega/\alpha & v_y/\alpha \\ -\alpha\omega & 0 & -\alpha v_x \\ (\alpha-1)v_y & (\alpha-1)v_x & 0 \end{bmatrix}. \tag{27}$$

Now observe that the basis (e_1, e_2, e_3) is orthogonal for the inner product induced by G because G is diagonal. Thus, the tangent plane to $S_F(1)$ in $\bar{u}_1$, denoted by A_1, is spanned by e_2 and e_3; and $J_{\bar{u}_1}|_{A_1}$ is the 2 by 2 sub-matrix of J_u composed of the two last columns and two last rows of (27). The same reasoning holds for the tangent plane A_2 (resp. A_3) in $\bar{u}_2$ (resp. $\bar{u}_2$) and we obtain

$$\begin{aligned} J_{\bar{u}_1}|_{A_1} &= \begin{bmatrix} 0 & -\alpha^{1/2} \\ \alpha^{-1/2}(\alpha-1) & 0 \end{bmatrix}, \\ J_{\bar{u}_2}|_{A_2} &= \begin{bmatrix} 0 & 1/\alpha \\ (\alpha-1) & 0 \end{bmatrix}, \quad J_{\bar{u}_3}|_{A_3} = \begin{bmatrix} 0 & 1/\alpha \\ -\alpha & 0 \end{bmatrix}. \end{aligned} \tag{28}$$

The Jacobians for $\bar{u}_4$, $\bar{u}_5$ and $\bar{u}_6$ are the opposite of the ones for $\bar{u}_1$, $\bar{u}_2$ and $\bar{u}_3$. The eigenvalues of those Jacobians are given by the roots of their characteristic polynomial (see Appendix E for details).

$J_{\bar{u}_1}|_{A_1}$ and $J_{\bar{u}_1}|_{A_1}$ have purely imaginary eigenvalues because $\alpha - 1 > 0$, thus, the real parts of the eigenvalues are zero. $\bar{u}_1$, $\bar{u}_3$, $\bar{u}_4$ and $\bar{u}_6$ are not saddle points. On the other hand, $J_{\bar{u}_2}|_{A_2}$ has eigenvalues $\pm\sqrt{(\alpha-1)/\alpha}$, of which one is positive while the other one is negative.

To conclude, $\bar{u}_2 = e_2$ and $\bar{u}_5 = -e_2$ are the only saddle points. These are precisely the two translations along the y axis of the local frame, i.e., parallel to the short side of the rectangle. Conjecture 1 implies that the left-invariant vector fields of instantaneous translations parallel to the short side are geodesic turnpikes. It is precisely the turnpike behavior observed in Fig. 1(bottom), hinting at the potential validity of the conjecture.

This section has shown a prototypical strategy to find the saddle points of the geodesic dynamics analytically. In the following subsection, we present a numerical strategy for identifying the saddle points for more general distances and a procedure for using them in the geodesic computation.

B. Geodesic turnpike for the minimum swept-volume distance

We propose a numerical procedure to accelerate the geodesic computation associated with F. First, an offline algorithm identifies the saddle points of the Lie algebra dynamics. Assuming Conjecture 1, they are geodesic turnpikes. Second, we propose an initialization strategy using the candidate geodesic turnpikes in a geodesic solver that significantly accelerates the convergence. It is important to note that the first part of the computation is done only once for a given Finsler operator F and not for every geodesic computation. Thus, identifying candidate geodesic turnpikes does not impact the computation cost of a specific geodesic joining a pair of configurations, as done in motion planners such as RRT and its variants [6].

We assume that F is a left-invariant Finsler operator known in closed form as a function of u, an element of the Lie algebra. It is the case for the minimum swept-volume distance [1] for a moving rod. Note that Figures 1, 2 and 3 illustrate geodesics computed with this operator. We use this example throughout the section and use the geodesic turnpikes to compute the same geodesics significantly faster.

Saddle points identification. We implement the symbolic expression of $F(e,u)$, $\mathrm{ad_u}$ and $\mathrm{P_u}$ in the symbolic automatic differentiation framework CasADi [32]. We use automatic differentiation to compute the symbolic expression of the hessian of F and, in turn, the symbolic expression of G_u, $D(u)$, and J_u. We use the non-linear root finding engine implemented in CasADi with multiple initializations to identify the roots of the system (18), i.e., the equilibrium points $\bar{u}_i$, and thus the numerical matrices $J_i = J_{\bar{u}_i}$. We use a sequence of matrix factorization routines detailed in Appendix F to compute the spectrum of the Jacobian restricted to the tangent plane of $S_F(1)$ in $\bar{u}_i$. We only keep the $\bar{u}_i$ that are saddle points.

When applied to the minimum swept-volume distance of a moving rod, this algorithm yields exactly two turnpikes: the instantaneous translation parallel to the long side of the rod in both directions. It is consistent with the turnpike behavior observed in Fig. 1 hinting again at the potential validity of the conjecture 1.

Initialization of the geodesic solver In [1], the geodesics are computed using a discretized version of the energy problem (7) with optimization variables (u_j) with $j = 0..N$. We adopt a two-stage approach. First, for each saddle point $\bar{u}_i$, we initialize the (u_j) with $u_j = \bar{u}_i$ for all j, and we solve the minimization problem with u_j fixed for $j = 1..N-1$ and only u_0 and u_N as optimization variables. Seco+nd, we keep the saddle point $\bar{u}_i$ with the lowest cost error and solve the associated minimization problem a second time with all u_j as optimization variables.

On an Intel(R) Core(TM) i7-8750H CPU, averaging over 100 cases, the first optimization problem takes $13ms$ to converge for each turnpike, and the second optimization problem takes around 110 ms. In comparison, the standard optimization used in [1] takes $1.5s$ to converge.

Overall, geodesic turnpike initialization improved the timings of geodesic computation by an order of magnitude over the standard geodesic solver used in [1].

V. Conclusion

This paper has laid a theoretical framework for exploring the geodesic turnpike properties for metric structures on configuration spaces. We introduced the notion of *exponential geodesic turnpikes*, and we propose a conjecture for a sufficient condition for a left-invariant Finsler operator to enjoy the geodesic turnpike property. The examples in section IV support the conjecture. In addition, using a geodesic turnpike as an initialization for the geodesic solver of the swept-volume distance [1] offers a significant acceleration. In future works, we will try to prove the conjecture. The reversibility of geodesics is expected to be the main property to exploit. Future work will also include an in-depth study of only partially invariant distances and further exploration of the implications of the turnpike property on various robotics applications.

Acknowledgments

This work was funded in part by the French government under management of Agence Nationale de la Recherche as 8 part of the "Investissements d'avenir" program, reference ANR-19-P3IA-0001 (PRAIRIE 3IA Institute). JP was supported in part by the Louis Vuitton/ENS-PSL chair in artificial intelligence and a Global Distinguished Professorship at the Courant Institute of Mathematical Sciences and the Center for Data Science at New York University.

References

[1] Y. de Mont-Marin, J. Ponce, and J.-P. Laumond, "A minimum swept-volume metric structure for configuration space," in *IEEE International Conference on Robotics and Automation (ICRA)*, pp. 3686–3692, 2023.

[2] E. Trélat and E. Zuazua, "The turnpike property in finite-dimensional nonlinear optimal control," *Journal of Differential Equations*, vol. 258, no. 1, pp. 81–114, 2015.

[3] M. Žefran, V. Kumar, and C. B. Croke, "On the generation of smooth three-dimensional rigid body motions," *IEEE Transactions on Robotics and Automation*, vol. 14, no. 4, pp. 576–589, 1998.

[4] G. S. Chirikjian, "Partial bi-invariance of $SE(3)$ metrics," *Journal of Computing and Information Science in Engineering*, vol. 15, no. 1, 2015.

[5] J. J. Kuffner, "Effective sampling and distance metrics for 3d rigid body path planning," *IEEE International Conference on Robotics and Automation (ICRA)*, vol. 2004, no. 4, pp. 3993–3998, 2004.

[6] S. M. LaValle, *Planning Algorithms*. Cambridge University Press, 2006.

[7] L. Palmieri and K. Arras, "Distance metric learning for rrt-based motion planning with constant-time inference," *IEEE International Conference on Robotics and Automation (ICRA)*, vol. 2015, 2015.

[8] L. Paiola, G. Grioli, and A. Bicchi, "On the evaluation of collision probability along a path," 2023.

[9] N. D. Ratliff, M. Zucker, J. A. Bagnell, and S. S. Srinivasa, "Chomp: Gradient optimization techniques for efficient motion planning," in *IEEE International Conference on Robotics and Automation (ICRA)*, IEEE, 2009.

[10] N. Jaquier, L. Rozo, and T. Asfour, "Unraveling the single tangent space fallacy: An analysis and clarification for applying riemannian geometry in robot learning," *ArXiv*, vol. abs/2310.07902, 2023.

[11] N. Jaquier and T. Asfour, "Riemannian geometry as a unifying theory for robot motion learning and control," in *Robotics Research* (A. Billard, T. Asfour, and O. Khatib, eds.), (Cham), pp. 395–403, Springer Nature Switzerland, 2023.

[12] H. Klein, N. Jaquier, A. Meixner, and T. Asfour, "A riemannian take on human motion analysis and retarget-

ing," in *IEEE/RSJ International Conference on Intelligent Robots and Systems (IROS)*, pp. 5210–5217, IEEE, 2022.
[13] N. D. Ratliff, K. Van Wyk, M. Xie, A. Li, and M. A. Rana, "Generalized nonlinear and finsler geometry for robotics," in *IEEE International Conference on Robotics and Automation (ICRA)*, pp. 10206–10212, 2021.
[14] K. Van Wyk, M. Xie, A. Li, M. A. Rana, B. Babich, B. Peele, Q. Wan, I. Akinola, B. Sundaralingam, D. Fox, B. Boots, and N. D. Ratliff, "Geometric fabrics: Generalizing classical mechanics to capture the physics of behavior," *IEEE Robotics and Automation Letters*, vol. 7, no. 2, pp. 3202–3209, 2022.
[15] L. W. McKenzie, "Turnpike theory," *Econometrica*, vol. 44, no. 5, pp. 841–865, 1976.
[16] N. Sakamoto and E. Zuazua, "The turnpike property in nonlinear optimal control–a geometric approach," *Automatica*, vol. 134, p. 109939, 2021.
[17] B. Geshkovski and E. Zuazua, "Turnpike in optimal control of pdes, resnets, and beyond," *Acta Numerica*, vol. 31, p. 135–263, 2022.
[18] C. Kuehn, *Multiple Time Scale Dynamics*. Applied Mathematical Sciences, Springer International Publishing, 2016.
[19] L. Zhang, Y. J. Kim, and D. Manocha, "C-DIST," in *ACM symposium on Solid and physical modeling (SPM)*, ACM Press, 2007.
[20] M. Žefran, V. Kumar, and C. B. Croke, "Choice of riemannian metrics for rigid body kinematics," *International Design Engineering Technical Conferences and Computers and Information in Engineering Conference (IDETC/CIE)*, vol. 2B-1996, no. 3, pp. 1–23, 1996.
[21] T. Faulwasser and L. Grüne, "Chapter 11 - turnpike properties in optimal control: An overview of discrete-time and continuous-time results," in *Numerical Control: Part A* (E. Trélat and E. Zuazua, eds.), vol. 23 of *Handbook of Numerical Analysis*, pp. 367–400, Elsevier, 2022.
[22] E. Frazzoli, M. A. Dahleh, and E. Feron, "Maneuver-based motion planning for nonlinear systems with symmetries," *IEEE Transactions on Robotics*, vol. 21, no. 6, pp. 1077–1091, 2005.
[23] I. Bucataru and R. Miron, *Finsler-Lagrange Geometry: Applications to Dynamical Systems*. Editura Academiei Române, 2007.
[24] R. Featherstone, *Rigid body dynamics algorithms*. New York: Springer, 2008.
[25] F. A. Potra and S. J. Wright, "Interior-point methods," *Journal of Computational and Applied Mathematics*, vol. 124, no. 1, pp. 281–302, 2000. Numerical Analysis 2000. Vol. IV: Optimization and Nonlinear Equations.
[26] W. Jallet, A. Bambade, N. Mansard, and J. Carpentier, "Constrained differential dynamic programming: A primal-dual augmented lagrangian approach," in *IEEE/RSJ International Conference on Intelligent Robots and Systems (IROS)*, pp. 13371–13378, 2022.
[27] J. Kierzenka and L. F. Shampine, "A bvp solver based on residual control and the maltab pse," *ACM Transaction on Mathematical Software*, vol. 27, no. 3, p. 299–316, 2001.
[28] G. S. Chirikjian, *Stochastic Models, Information Theory and Lie Groups Volume 2, Analytic Mehods and Modern Applications*. Birkhäuser Boston, 2012.
[29] V. I. Arnol'd, *Mathematical methods of classical mechanics*. Graduate Texts in Mathematics, New York, NY: Springer, 2 ed., 1989.
[30] E. Celledoni, H. Marthinsen, and B. Owren, "An introduction to lie group integrators – basics, new developments and applications," *Journal of Computational Physics*, vol. 257, pp. 1040–1061, 2014. Physics-compatible numerical methods.
[31] D. Latifi and A. Razavi, "Bi-invariant finsler metrics on lie groups," *Australian Journal of Basic and Applied Science*, vol. 5, no. 12, pp. 507–511, 2011.
[32] J. A. E. Andersson, J. Gillis, G. Horn, J. B. Rawlings, and M. Diehl, "Casadi: a software framework for nonlinear optimization and optimal control," *Mathematical Programming Computation*, vol. 11, no. 1, p. 1–36, 2018.
[33] A. L. Onishchik and E. B. Vinberg, *Lie Groups and Algebraic Groups*. Springer Berlin Heidelberg, 1990.
[34] V. R. Kjer, "Lie group integrators for cotangent bundles of lie groups and their application to systems of dipolar soft spheres," Oslo, Norway, 2022. Under supervision of Brynjulf, Owren, IMF.
[35] J. Solà, J. Deray, and D. Atchuthan, "A micro lie theory for state estimation in robotics," *ArXiv*, vol. abs/1812.01537, 2018.

APPENDIX

A. Proof of Finsler operator properties

We will prove five properties of the Finslerian operator F and the associated bilinear form g as defined in (10). The ones mentioned in section II are properties A.1, A.2, A.5.

Property A.1. *For any x in X and v in T_xX we have $F^2(x,v) = g(x,v)(v,v)$.*

Proof: Using the definition

$$\begin{aligned} g(x,v)(v,v) &= \frac{1}{2}\frac{\partial^2}{\partial s \partial t} F^2(x, v+sv+tv)\Big|_{s=0,t=0} \\ &= \frac{\partial^2}{\partial s \partial t}\frac{1}{2}(1+s+t)^2\Big|_{s=0,t=0} F^2(x,v) \\ &= F^2(x,v). \end{aligned} \tag{29}$$

■

Property A.2. *For any x in X, v in T_xX and $\lambda > 0$ we have*

$$g(x, \lambda v) = g(x,v). \tag{30}$$

Proof: For any a and b in T_xX we have

$$\begin{aligned} g(x,\lambda v)(a,b) &= \frac{1}{2}\lim_{s\to 0^+, t\to 0^+} \frac{F^2(x, \lambda v + sa + tb)}{st} \\ &= \frac{1}{2}\lim_{s\to 0^+, t\to 0^+} \frac{\lambda^2 F^2(x, v + (s/\lambda)a + (t/\lambda)b)}{\lambda^2 (s/\lambda)(t/\lambda)} \\ &= \frac{1}{2}\lim_{s'\to 0^+, t'\to 0^+} \frac{F^2(x, v + s'a + t'b)}{s't'} \\ &= g(x,v)(a,b), \end{aligned} \tag{31}$$

where we use the changes of variables $s' = s/\lambda$ and $t' = t/\lambda$. ■

Property A.3. *We denote by C the tri-linear symmetric form called the Cartan tensor [23] defined for any a,b,c in T_xX as*

$$C(x,v)(a,b,c) = \frac{1}{2}\frac{\partial^3}{\partial s \partial t \partial u} F^2(x, v+sa+tb+uc)\Big|_{s=0,t=0,u=0}. \tag{32}$$

For any x in X and v,a,b in T_xX we have

$$C(x,v)(v,a,b) = 0. \tag{33}$$

Proof:

$$\begin{aligned} C(x,v)(v,a,b) &= \frac{1}{2}\frac{\partial^3}{\partial s \partial t \partial u} F^2(x, v+sv+ta+ub)\Big|_{s=0,t=0,u=0} \\ &= \frac{\partial}{\partial s}\left[\frac{1}{2}\frac{\partial^2}{\partial t \partial u} F^2(x, (1+s)v+ta+ub)\Big|_{t=0,u=0}\right]_{s=0} \\ &= \frac{\partial}{\partial s} g(x, (1+s)v)(a,b)\Big|_{s=0} \\ &= \frac{\partial}{\partial s} g(x,v)(a,b)\Big|_{s=0} \qquad (34) \\ &= 0, \qquad (35) \end{aligned}$$

where we used the property A.2 between the second to last and last equality. ■

Property A.4. *For any x in X and v,a,b in T_xX we have*

$$\frac{\partial}{\partial s} g(x, v+sa)(v,b)\Big|_{s=0} = 0, \tag{36}$$

Proof: We have $\frac{\partial}{\partial s} g(x, v+sa)(v,b)\Big|_{s=0} = C(x,v)(v,a,b)$ hence the result using property A.3. ∎

Property A.5. *For any x in X and v, w in T_xX we have*

$$\frac{1}{2}\frac{\partial}{\partial s} F^2(x, v+sw)\Big|_{s=0} = g(x,v)(v,w). \tag{37}$$

Proof: Using the property A.1, we have

$$\begin{aligned} F^2(x, v+sw) &= g(x, v+sw)(v+sw, v+sw) \\ &= g(x, v+sw)(v,v) + 2sg(x, v+sw)(v,w) + s^2 g(x, v+sw)(w,w). \end{aligned} \tag{38}$$

Taking the derivative with respect to s, we have

$$\begin{aligned} \frac{\partial}{\partial s} F^2(x, v+sw) = &\frac{\partial}{\partial s} g(x, v+sw)(v,v) && \text{(39a)} \\ &+ 2g(x, v+sw)(v,w) && \text{(39b)} \\ &+ 2s\frac{\partial}{\partial s} g(x, v+sw)(v,w) && \text{(39c)} \\ &+ 2sg(x, v+sw)(w,w) && \text{(39d)} \\ &+ s^2 \frac{\partial}{\partial s} g(x, v+sw)(w,w). && \text{(39e)} \end{aligned}$$

When $s=0$ (39c), (39d), (39e) are naturally equal to 0 and using property A.4 the term (39a) is also equal to 0. Only (39b) is not zero, and we obtain

$$\frac{\partial}{\partial s} F^2(x, v+sw)\Big|_{s=0} = g(x,v)(v,w) \tag{40}$$

Hence, the final result. ∎

In the rest of the appendices, given a map $f : \mathfrak{X} \times Y \to Z$ with Y a manifold and Z a vector space, for any u in X, y in Y we denote by $\frac{\partial}{\partial u} f\Big|_{u,y}$ the linear map from $\mathfrak{X}$ onto Z defined for any v in $\mathfrak{X}$ as

$$\frac{\partial}{\partial u} f\Big|_{u,y} v = \frac{\partial}{\partial s} f(u+sv, y)\Big|_{s=0}. \tag{41}$$

B. Proof of proposition 5

Proposition. *For any $\varepsilon > 0$, there exists $\tau > 0$ such that for any curvilinear parametric curve $\gamma^\dagger$ representing a geodesic, if I_ε denote the interval of t such that $F\left(\gamma^\dagger(t), \dot\gamma^\dagger(t) - V_{\gamma^\dagger(t)}\right) \geq \varepsilon$ we have*

$$L\left(\gamma^\dagger|_{I_\varepsilon}\right) \leq \tau. \tag{14}$$

Proof: Let $\gamma^\dagger$ a parametric curve representing a geodesic joining x_0 to x_1 with constant velocity and of length, $L = d(x_0, x_1)$ verifying Definition 1. For any $\varepsilon > 0$ we chose $\tau = (2/\sigma)\ln(2K/\varepsilon)$, which is independent of the length L and we verify:

- for any $t > \tau/2$ we have $e^{-\sigma t} < e^{-\sigma\frac{\tau}{2}} = e^{-\ln(2K/\varepsilon)} = \varepsilon/(2K)$,
- for any $t < L - \tau/2$ we have $e^{-\sigma(L-t)} < e^{-\sigma(L-(L-\frac{\tau}{2})} = e^{-\sigma\frac{\tau}{2}} = \varepsilon/(2K)$.

Summing up, we have

$$\left(\gamma^\dagger(t), \dot\gamma^\dagger(t) - V_{\gamma^\dagger(t)}\right) \leq K\left(e^{-\sigma t} + e^{-\sigma(L-t)}\right) \leq \varepsilon \quad , \quad t \in [\tau/2, L] \cap [0, L-\tau/2]. \tag{42}$$

Thus, if I_ε denote the interval of t such that $F\left(\gamma^\dagger(t), \dot\gamma^\dagger(t) - V_{\gamma^\dagger(t)}\right) > \varepsilon$ we have

$$I_\varepsilon \subset [0,L] \setminus ([\tau/2, L] \cap [0, L-\tau/2]) \subset [0, \tau/2] \cup [L-\tau/2, L], \tag{43}$$

and $\mu(I_\varepsilon) \leq \mu([0,\tau/2]) + \mu([0,\tau/2]) = \tau$, hence the result. ∎

C. Proof of proposition 6

Proposition. *If F is a left-invariant Finsler distance on the Lie group X, then the geodesic equation associated to* (16) *can be written in some basis of $\mathfrak{X}$:*

$$\begin{aligned}\dot{\gamma}(t) &= \tilde{L}_{\gamma(t)}u(t),\\ \dot{u}(t) &= G_{u(t)}^{-1}\,\mathrm{ad}_{u(t)}^{\top}\,G_{u(t)}u(t),\end{aligned} \tag{17}$$

where G_u denote the matrix representation of $g(e,u)$ in the chosen basis and ad_u denote the matrix representation of the adjoint operator of u on $\mathfrak{X}$ in the chosen basis. The solutions represent local geodesics and do not depend on the basis choice.

Proof: The Hamiltonian of the variational problem (16) reads

$$H(x,p,u) = < p, \tilde{L}_x u >_x - C(u), \tag{44}$$

where and $u \in \mathfrak{X}$ and $(x,p) \in T^*X$ the co-tangent of X, i.e., $x \in X$ and p is a linear form on T_xX. $< p, v >_x$ is the dual bracket that takes a covector and a vector and returns the scalar obtained by applying the covector on the vector on the tangent space in x. The cotangent bundle T^*X of a Lie group X is a trivial bundle[1], and the Hamiltonian equations for all t are:

$$\dot{x}(t) = \left.\frac{\partial H}{\partial p}\right|_{x(t),p(t),u(t)} = \tilde{L}_{x(t)}u(t), \tag{45a}$$

$$\dot{p}(t) = -\left.\frac{\partial H}{\partial x}\right|_{x(t),p(t),u(t)} = -\left.\frac{\partial < p, \tilde{L}_x u >_x}{\partial x}\right|_{x(t),p(t),u(t)}, \tag{45b}$$

$$0 = \left.\frac{\partial H}{\partial u}\right|_{x(t),p(t),u(t)} = \left.\frac{\partial < p, \tilde{L}_x u >_x}{\partial u}\right|_{x(t),p(t),u(t)} - \left.\frac{\partial C}{\partial u}\right|_{u(t)}. \tag{45c}$$

We use the left trivialization of the cotangent bundle described below to simplify the Hamiltonian equations. For (x,p) in T^*X, we denote by $p_b = p \circ \tilde{L}_x \in \mathfrak{X}^*$ the left trivialization of the covector p. The cotangent bundle, T^*X, is equipped with a natural group structure induced by the group structure of X (see [33, 34] for details) and the mapping

$$\phi : (x,p) \in T^*X \mapsto (x, p_b) \in X \ltimes \mathfrak{X}^*, \tag{46}$$

is a Lie group isomorphism where $X \ltimes \mathfrak{X}^*$ is a lie-group semi-direct product with the group law

$$(x, p_b) \circ (y, q_b) = (x \circ y, \mathrm{Ad}_y^*(p_b) + q_b), \tag{47}$$

where Ad_y^* is the co-adjoint representation of $y \in X$ (see [33] for details).
First, we have $< p, \tilde{L}_x u >_x = < p \circ \tilde{L}_x, u >_e = < p_b, u >_e$ and the third Hamiltonian equation (45c) is equivalent to:

$$\begin{aligned} 0 &= \left.\frac{\partial < p_b, u >_e}{\partial u}\right|_{x(t),p(t),u(t)} - \left.\frac{\partial C}{\partial u}\right|_{u(t)},\\ p_b(t) &= \left.\frac{\partial C}{\partial u}\right|_{u(t)}. \end{aligned} \tag{48}$$

Second, we denote by $\pi : (x, p_b) \in X \ltimes \mathfrak{X}^* \to p_b$ the projection, and we use the left Jacobian, as coined in [35], for v in $\mathfrak{X}$ we have

$$\begin{aligned} \frac{\partial \pi}{\partial x}(\tilde{L}_x v) &= \left.\frac{\partial}{\partial s}\pi((x,p_b) \circ (\exp(sv), 0))\right|_{s=0}\\ \frac{\partial p_b}{\partial x}(\tilde{L}_x v) &= \left.\frac{\partial}{\partial s}\,\mathrm{Ad}^*_{\exp(sv)}(p_b) + 0\right|_{s=0}\\ &= \left.\frac{\partial}{\partial s}\exp(s\,\mathrm{ad}_v^*)\right|_{s=0}(p_b)\\ &= \mathrm{ad}_v^*(p_b). \end{aligned} \tag{49}$$

We denote by ψ the linear form on $\mathfrak{X}$ defined as

$$\psi = -\frac{\partial < p_b, u >_e}{\partial x} \circ \tilde{L}_x, \tag{50}$$

[1] its topology is the one of a Cartesian product between the base space X and a fiber

for any $v \in \mathfrak{X}$ we have

$$\begin{aligned}\psi(v) &= - < \frac{\partial p_b}{\partial x}(\tilde{L}_x v), u >_e \\ &= - < \mathrm{ad}^*_v(p_b), u >_e \\ &= - < p_b, \mathrm{ad}_v(u) >_e \\ &= < p_b, \mathrm{ad}_u(v) >_e \\ &= < \mathrm{ad}^*_u(p_b), v >_e, \end{aligned} \tag{51}$$

and we conclude that $\psi = \mathrm{ad}^*_u(p_b)$. Composing the second Hamiltonian equation (45b) on both side with $\tilde{L}_x$, the second Hamiltonian equation is equivalent to

$$\begin{aligned}\dot{p_b} &= -\frac{\partial < p, \tilde{L}_x u >_x}{\partial x} \circ \tilde{L}_x \\ &= -\frac{\partial < p_b, xu >_e}{\partial x} \circ \tilde{L}_x \\ &= \mathrm{ad}^*_u(p_b). \end{aligned} \tag{52}$$

Third, substituting (48) in (52), the Hamiltonian equations (45a), (45b), (45c) are rewritten as

$$\dot{x}(t) = \tilde{L}_{x(t)} u(t), \tag{53a}$$

$$\left.\frac{\partial^2 C}{\partial^2 u}\right|_{u(t)} \dot{u}(t) = \mathrm{ad}^*_{u(t)} \left(\left.\frac{\partial C}{\partial u}\right|_{u(t)} \right). \tag{53b}$$

Note that the right and left sides are in $\mathfrak{X}^*$. Note also that the previous construction is valid for any invariant cost C. Now, using the definition of g in (10) and the property A.5, we have

$$\left.\frac{\partial^2}{\partial^2 u} C\right|_u (v, w) = g(e,u)(v,w), \tag{54a}$$

$$\left.\frac{\partial}{\partial u} C\right|_u (v) = g(e,u)(u,v). \tag{54b}$$

Using a basis of $\mathfrak{X}$ and its dual basis, we identify elements of $\mathfrak{X}^*$ and $\mathfrak{X}$. G_u is the matrix representation in this basis of $\left.\frac{\partial^2 C}{\partial^2 u}\right|_{u(t)}$, and $\mathrm{ad}^\top$ is the basis representation of ad^*. Finally, we have the geodesic equation:

$$\dot{x}(t) = \tilde{L}_{x(t)} u(t), \tag{55a}$$

$$G_{u(t)} \dot{u}(t) = \mathrm{ad}^\top_{u(t)} G_{u(t)} u(t), \tag{55b}$$

hence the result. ∎

D. Details on Section III-D

Section III-D analyzes the dynamics of the geodesic equation to identify saddle points. In this section, we prove the results stated without proof in III-D. We recall the expression of the dynamics:

$$D(u) = G_u^{-1} \mathrm{ad}^\top_u G_u u. \tag{56}$$

Property D.1. *If $u : I \to \mathfrak{X}$ is a solution of $\dot{u} = D(u)$ then*

$$\frac{d}{dt} C(u) = 0. \tag{57}$$

Proof: A solution of the dynamics $\dot{u} = D(u)$ verifies

$$u^\top G_u \dot{u} = u^\top \mathrm{ad}^\top_u G_u u = (\mathrm{ad}_u u)^\top G_u u = 0, \tag{58}$$

because the mapping $u, v \mapsto \mathrm{ad}_u v$ is antisymmetric and we have $\mathrm{ad}_u u = 0$. Now, using (37) we obtain

$$\frac{d}{dt} C(u) = \left.\frac{\partial}{\partial u} C\right|_u \dot{u} = g(e,u)(u,\dot{u}) = u^\top G_u \dot{u} = 0, \tag{59}$$

hence the result. ∎

The dynamics solutions have constant cost C and, in turn, constant Finsler operator $F(e,u)$. We restrict the dynamics domain to $S_F(1)$, the set of all u such that $F(e,u) = 1$.

Property D.2. *A vector $\bar{u}$ is an equilibrium point of the dynamics D defined on $S_F(1)$ if:*

$$\mathrm{ad}_{\bar{u}}^\top G_{\bar{u}}\bar{u} = 0, \quad \bar{u}^\top G_{\bar{u}}\bar{u} = 1, \tag{18}$$

Proof: First, an equilibrium point verifies $D(\bar{u}) = 0$. With (56) and canceling the invertible matrix G_u, we obtain the left part of (18). Second, using property A.1, $S_F(1)$ is exactly the set of u such that $g(e,u)(u,u) = u^\top G_u u = 1$ hence the result. ■

Property D.3. *Let J_u denote the Jacobian of the dynamics D taken in u. If $\bar{u}$ is an equilibrium point of the dynamics, then we have*

$$J_{\bar{u}} = G_{\bar{u}}^{-1}(\mathrm{ad}_{\bar{u}}^\top G_{\bar{u}} + \mathrm{P}_{G_{\bar{u}}\bar{u}}). \tag{20}$$

Proof: Taking the derivative of D defined in (56), we have

$$J_u v = \left[\frac{\partial}{\partial u} G_u^{-1}\bigg|_u v\right] \mathrm{ad}_u^\top G_u u \tag{60a}$$
$$+ G_u^{-1}\,\mathrm{ad}_v^\top G_u u \tag{60b}$$
$$+ G_u^{-1}\,\mathrm{ad}_u^\top \left[\frac{\partial}{\partial u} G_u\bigg|_u v\right] u \tag{60c}$$
$$+ G_u^{-1}\,\mathrm{ad}_u^\top G_u v. \tag{60d}$$

The term (60c) is zero because $\left[\frac{\partial}{\partial u} G_u\Big|_u v\right] u$ is the transpose of the matrix representation of the linear mapping $w \in \mathfrak{X} \to \frac{\partial}{\partial s} g(e, u+sv)(u,w)\Big|_{s=0}$ which is zero as stated in Property A.4. Using $\mathrm{ad}_v^\top G_u u = \mathrm{P}_{G_u u} v$ with P defined in (19) and identifying D we obtain

$$J_u v = \left[\frac{\partial}{\partial u} G_u^{-1}\bigg|_u v\right] G_u D(u) + G_u^{-1}(\mathrm{P}_{G_u u} + \mathrm{ad}_u^\top G_u) v. \tag{61}$$

Hence with $\bar{u}$ an equilibrium point, i.e., $D(\bar{u}) = 0$ we have

$$J_{\bar{u}} = G_{\bar{u}}^{-1}(\mathrm{ad}_{\bar{u}}^\top G_{\bar{u}} + \mathrm{P}_{G_{\bar{u}}\bar{u}}). \tag{62}$$

■

Property D.4. *The tangent space to $S_F(1)$ in u, denoted by $T_u S_F(1)$, is the vector space of element v in $\mathfrak{X}$ such that $v^\top G_u u = 0$.*

Proof: We have that $S_F(1) = S_C(1/2)$, i.e., $S_F(1)$ is a level set of C. Thus, for u in $S_F(1)$ the tangent space $T_u S_F(1)$ is the set of vector v in the kernel of the differential of C in u:

$$\frac{\partial}{\partial u} C\bigg|_u v = 0,$$
$$g(e,u)(u,v) = u^\top G_u v = 0, \tag{63}$$

using property A.4. ■

E. Details on Section IV-A

Detailed derivation of the operators

This section details the derivation of the expression of $\mathrm{ad}_u, \mathrm{P}_u, J_u, \mathrm{ad}_u^\top G_u u$ when $X = \mathrm{SE}(2)$, the group of rigid transformation of $\mathbb{R}^2$. SE(2) has a canonic matrix Lie group representation with the set of matrix M written as

$$M = \begin{pmatrix} cos(\theta) & -sin(\theta) & x \\ sin(\theta) & cos(\theta) & y \\ 0 & 0 & 1 \end{pmatrix}, \tag{64}$$

with parameter θ, x, y. We use parenthesis for the elements of the matrix group to distinguish them from the matrix written with brackets representing endomorphisms of the lie algebra. The identity matrix, i.e., the identity element of the group, is obtained with $\theta = 0, x = 0, y = 0$. Taking the derivative of M with respect to the parameters at $0,0,0$, we obtain a lie algebra element m written as

$$m = \begin{pmatrix} 0 & -\omega & v_x \\ \omega & 0 & v_y \\ 0 & 0 & 0 \end{pmatrix} = v_x e_1 + v_y e_2 + \omega e_3, \tag{65}$$

$$\text{with} \quad e_1 = \begin{pmatrix} 0 & 0 & 1 \\ 0 & 0 & 0 \\ 0 & 0 & 0 \end{pmatrix}, \quad e_2 = \begin{pmatrix} 0 & 0 & 0 \\ 0 & 0 & 1 \\ 0 & 0 & 0 \end{pmatrix}, \quad e_3 = \begin{pmatrix} 0 & -1 & 0 \\ 1 & 0 & 0 \\ 0 & 0 & 0 \end{pmatrix},$$

and (e_1, e_2, e_3) is the canonical basis of the lie algebra. We denote by $u = [v_x, v_y, \omega]$ the column vector associated to m and $u' = [v'_x, v'_y, \omega']$ the column vector associated to m' another element of the lie algebra. The adjoint operator on a matrix lie group is the matrix commutator:

$$[m, m'] = mm' - m'm = \begin{pmatrix} 0 & 0 & (-\omega v'_y) - (-\omega' v_y) \\ 0 & 0 & (\omega v'_x) - (\omega' v_x) \\ 0 & 0 & 0 \end{pmatrix} = (-\omega v'_y + v_y \omega')e_1 + (\omega v'_x - v_x \omega')e_2 + 0e_3. \tag{66}$$

Thus, the representation of the adjoint operator associated with the basis (e_1, e_2, e_3) denoted by ad_u must verify $\mathrm{ad}_u u' = [-\omega v'_y + v_y \omega', \omega v'_x - v_x \omega', 0]^\top$ and we have

$$\mathrm{ad}_u = \begin{bmatrix} 0 & -\omega & v_y \\ \omega & 0 & -v_x \\ 0 & 0 & 0 \end{bmatrix}. \tag{67}$$

We calculate

$$\mathrm{ad}_u^\top u' = \begin{bmatrix} 0 & \omega & 0 \\ -\omega & 0 & 0 \\ v_y & -v_x & 0 \end{bmatrix} \begin{bmatrix} v'_x \\ v'_y \\ \omega' \end{bmatrix} = \begin{bmatrix} v'_y \omega \\ -v'_x \omega \\ -v'_y v_x + v'_x v_y \end{bmatrix} = \begin{bmatrix} 0 & 0 & v'_y \\ 0 & 0 & -v'_x \\ -v'_y & v'_x & 0 \end{bmatrix} \begin{bmatrix} v_x \\ v_y \\ \omega \end{bmatrix} = \mathrm{P}_{u'} u, \tag{68}$$

and we obtain

$$\mathrm{P}_u = \begin{bmatrix} 0 & 0 & v_y \\ 0 & 0 & -v_x \\ -v_y & v_x & 0 \end{bmatrix}. \tag{69}$$

Now recall that

$$G = \begin{bmatrix} \alpha & 0 & 0 \\ 0 & 1 & 0 \\ 0 & 0 & 1 \end{bmatrix}, \tag{70}$$

and substituting the previous expressions in (18) and (20) we obtain

$$\mathrm{ad}_u^\top G_u u = \begin{bmatrix} 0 & \omega & 0 \\ -\omega & 0 & 0 \\ v_y & -v_x & 0 \end{bmatrix} \begin{bmatrix} \alpha v_x \\ v_y \\ \omega \end{bmatrix} = \begin{bmatrix} v_y \omega \\ -\alpha v_x \omega \\ (\alpha - 1) v_x v_y \end{bmatrix}, \tag{71a}$$

$$u^\top G_u u = \alpha v_x^2 + v_y^2 + \omega^2 \tag{71b}$$

$$\begin{aligned} J_u = G_u^{-1} \mathrm{ad}_u^\top G_u + G_u^{-1} \mathrm{P}_{G_u u} &= \begin{bmatrix} 0 & \omega/\alpha & 0 \\ -\alpha\omega & 0 & 0 \\ \alpha v_y & -v_x & 0 \end{bmatrix} + \begin{bmatrix} 1/\alpha & 0 & 0 \\ 0 & 1 & 0 \\ 0 & 0 & 1 \end{bmatrix} \begin{bmatrix} 0 & 0 & v_y \\ 0 & 0 & -\alpha v_x \\ -v_y & \alpha v_x & 0 \end{bmatrix} \\ &= \begin{bmatrix} 0 & \omega/\alpha & v_y/\alpha \\ -\alpha\omega & 0 & -\alpha v_x \\ (\alpha - 1) v_y & (\alpha - 1) v_x & 0 \end{bmatrix}. \end{aligned} \tag{71c}$$

Detailed derivation of the saddle points

In this subsection, we detail how to compute the saddle points. The equation $\mathrm{ad}_u^\top G_u u = 0$ yields $v_x \omega = 0$, $v_y \omega = 0$ and $v_x v_y = 0$, and a solution $\bar{u}$ is a linear scaling of one of the vectors e_1, e_2, e_3. And $u^\top G_u u = 1$ yields six solutions:

$$\begin{aligned} &\bar{u}_1 = \alpha^{-1/2} e_1, \quad \bar{u}_2 = e_2, \quad \bar{u}_3 = e_3, \\ &\bar{u}_4 = -\alpha^{-1/2} e_1, \quad \bar{u}_5 = -e_2, \quad \bar{u}_6 = -e_3. \end{aligned} \tag{72}$$

We have

$$\begin{aligned} &\bar{u}_1^\top G e_2 = \bar{u}_1^\top G e_3 = 0, \\ &A_1 = T_{\bar{u}_1} S_F(1) = \mathrm{span}(e_2, e_3), \end{aligned} \tag{73}$$

and similar results with $\bar{u}_i, A_i$ for $i = 2..6$. Thus, we obtain

$$J_{\bar{u}_1}|_{A_1} = \begin{bmatrix} 0 & -\alpha^{1/2} \\ \alpha^{-1/2}(\alpha - 1) & 0 \end{bmatrix}, \tag{74}$$

$$J_{\bar{u}_2}|_{A_2} = \begin{bmatrix} 0 & 1/\alpha \\ (\alpha - 1) & 0 \end{bmatrix}, \quad J_{\bar{u}_3}|_{A_3} = \begin{bmatrix} 0 & 1/\alpha \\ -\alpha & 0 \end{bmatrix},$$

and $J_{\bar{u}_4}|_{A_4} = -J_{\bar{u}_1}|_{A_1}$, $J_{\bar{u}_5}|_{A_5} = -J_{\bar{u}_2}|_{A_2}$, $J_{\bar{u}_6}|_{A_6} = -J_{\bar{u}_3}|_{A_3}$. Now, denoting $P_i(x) = \det(J_{\bar{u}_i}|_{A_i} - x\mathrm{I}_2)$ the characteristic polynomial, we calculate

$$P_1(x) = x^2 + (\alpha - 1), \quad P_2(x) = x^2 - \frac{1}{\alpha}(\alpha - 1), \quad P_3(x) = x^2 + 1, \tag{75}$$

and $P_4 = P_1$, $P_5 = P_2$, $P_6 = P_3$. Only P_2 has real roots $\pm\sqrt{(\alpha-1)/\alpha}$ and only $\bar{u}_2, \bar{u}_5$ are saddle points.

F. Details on Section IV-B

Algorithm 1 Saddle points computation (see Appendix F)

Require: u ▷ A symbolic variable of dimension n
Require: $A : u \to F(e,u), B : u \to \mathrm{ad}_u, P : u \to P_u$
$G \leftarrow hessian(A)$ ▷ G is a symbolic expression
$D \leftarrow B^\top @G@u$ ▷ D is a symbolic expression
$C \leftarrow u^\top @G@u - 1$ ▷ C is a symbolic expression
$c \leftarrow []$
while $l \leq L$ **do** ▷ Multiple initialization
  $r \leftarrow root([D,C], gauss(0,1,n))$ ▷ eq is a numerical value
  $M \leftarrow apply(G,r)$
  $J \leftarrow M^{-1}(apply(B,r)@M + apply(P,M@r))$
  $A \leftarrow cholesky(M)$
  $A \leftarrow A^{-\top}@gramm(A^\top @complete(r))$
  $A \leftarrow pinv(A[1:])@J@A[1:]$
  $s \leftarrow diagonalization(A)$
  $c \leftarrow addif(c,s)$
  $l \leftarrow l + 1$
end while
return c

- @ denotes the matrix multiplication,
- $gauss(0,1,n)$ is a random vector of size n following a Gaussian distribution with 0 mean and 1 standard deviation,
- $root([C,D], u0)$ is a non-linear root solver for the combined expressions C and D in the symbolic variable u and taking an initial guess $u0$,
- $complete(r)$ return an invertible square matrix of size n with the first column being r,
- $cholesky(M)$ is the Cholesky decomposition of a symmetric positive definite matrix M,
- $gramm(M)$ return the matrix Q of the QR-decomposition. It corresponds to the matrix where columns the basis obtained with the Gram-Schmidt procedure,
- $A = A^{-\top} gramm(A^\top M)$ is a trick to compute the basis obtained with the Gram-Schmidt procedure using the inner product $u, v \to u^\top G v$ with $G = AA^\top$ instead of the canonical one,
- $A[1:]$ is a basis of the tangent space to $S_F(1)$ in e,
- $pinv(A[1:])$ is the Moore-Penrose pseudo inverse of $A[1:]$ it correspond to the inverse of $A[1:]|_{\mathrm{Im}(A[1:])}$,
- Using $A[1:]$ and its pseudo-inverse, we construct the square matrix $J|_{T_r S_F(1)}$ of size $n-1$ corresponding to the matrix J express in the base $A[1:]$.